Innovative Tools for Offshore Wind and DC Grids

Deliverable 2.3 – Work Package 2
Report on Optimal Control, Resonance Mitigation and System Configuration, Tool for Technical and Economic Analysis of Different Transmission Technologies Combined with Different Collection Concepts

WP2 Leader	DTU
Dissemination Level	Public
Website	https://innodc.org/
Grant Agreement Number	765585
Due Delivery	Month 24 - 31 AUG 2019
Project Period	01/09/2017 – 31/08/2021

Co-Authors

ESR 2	Gayan Abeynayake
ESR 9	Jovana Dakic
ESR 10	Anup Kavimandan
WP2 Leader	Nicolaos Antonio Cutululis

Summary

This report is intended as a summary of the research performed to date by Work Package 2 (WP2) of the InnoDC project. This report discusses about different offshore wind power plant cluster control architectures, resonance mitigation techniques, DC collection systems together with DC transformer concept. Following this, design possibilities for Offshore Wind Power Plants (OWPP) collector and transmission topologies considering High Voltage Alternating Current (HVAC), High Voltage Direct Current (HVDC) and Low Frequency Alternating Current (LFAC) are presented.

Section 1 discusses about control of large-scale OWPPs. It has historically been handled by separating the control into different hierarchical levels. A wind power plant control is traditionally implemented as a centralised processing unit. In case of large-scale OWPP clusters with hundreds of wind turbines , the centralised control scheme may be impractical owing to the huge computation burden in order to process the large volume of information. This chapter describes the need to breakdown the control problem into manageable sub-problems such that the overall plant is no longer controlled by a single controller, but by several independent controllers, giving rise to two additional control architectures - distributed and decentralized control. The resulting behaviour is the aggregated response of all the local independent controllers.

Section 2 highlights system configurations for DC collection systems. DC/DC converter and DC Circuit Breaker (DCCB) are two of the major components in any DC collection system. The development and design of an eligible concept, for a highly efficient and cost-effective DC/DC converter is essential for a DC collection system to be realized in the future. In the last section, a detailed overview of DC Wind Turbine (dcWT) concept is discussed with different dcWT topologies. Finally, possible control modes are discussed over conventional AC Wind Turbine (acWT).

Section 3 introduces cost modelling for different transmission systems. Already well-known HVAC and HVDC transmission systems are described and the cost functions are updated. LFAC system is analyzed as it is considered as a young non-industrialized technology. Capital investment costs and cost of losses are done separately. The result of this section is to allow a fair comparison between these systems.

Contents

Acronyms

AC	Alternating Current
acWT	AC Wind Turbine
B2B	Back to Back
DAB	Dual Active Bridge
DC	Direct Current
DCCB	DC Circuit Breaker
dcWT	DC Wind Turbine
DFIG	Doubly Fed Induction Generator
GSC	Grid Side Converter
HV	High Voltage
HVAC	High Voltage Alternating Current
HVDC	High Voltage Direct Current
IGBT	Insulated Gate Bi-polar Transistor
LCC	Line Commutated Converter
LFAC	Low Frequency Alternating Current
MMC	Modular Multi-Level Converter
MVdc	Medium Volatge dc
OWPP	Offshore Wind Power Plants
PMSG	Permanent Magnet Synchronous Generator
PWM	Pulse Width Modulation
RSC	Rotor Side Converter
SAB	Single Active Bridge
SSCB	Solid-State DC Circuit Breakers
STATCOM	Static Synchronous Compensator
TSO	Transmission System Operator
VSC	Voltage Source Converter
WECU	Wind-Energy Conversion Units
WPP	Wind Power Plant
XLPE	Cross Linked Polyethylene

1 Wind Power Plant Cluster Control Architectures

Written by Anup Kavimandan - DTU, Denmark

1.1 Introduction

Wind turbine controllers today are fully developed and most of them are optimized from a control perspective as a single wind turbine. Earlier there were single wind turbine generators which were aggregated under a Wind Power Plant (WPP) [1]. Nowadays, WPPs are being grouped together resulting in the formation of 'clusters' aggregated physically, connected to the same transmission grid node and controlled from an 'upper' level in the hierarchy. A wind power plant cluster is thus an electrical aggregation of independent physical offshore WPPs geographically existing in close proximity connected to the same grid node.

An OWPP cluster control architecture would typically consist of three levels: local wind turbine control, WPP control and control of group of WPPs to regulate the OWPP cluster power production to the reference power ordered by the system. In order to efficiently perform the monitoring and control of large OWPP clusters, a multilayer hierarchical control structure can be adopted so that the control responsibilities are assigned to the different hierarchical control levels such as the wind farm control architecture designed and implemented by A D Hansen et al. [2]. Alejandro J Gesino [3] defines a control strategy for a WPP cluster with the aim to receive a command sent by the Transmission System Operator (TSO) and calculate the set points to be sent to each WPP within the cluster in order to fulfil the grid requirements of the TSO. Making use of wind farm control strategies and wind energy forecast technologies, a Wind Farm Cluster Management System (WCMS) is developed [4] to perform active and reactive power control, congestion management, voltage as well as power factor control. The architecture, consisting of two layers, namely the 'TSO layer' and the 'dispatch layer', allows to efficiently monitor all wind farms operating in their control zones as well as reliably distribute control commands to all wind farms in the cluster.

Broadly speaking, the control architecture could typically be based upon one of the three types of control - centralised, distributed or decentralized control, each of them being characterized by the flow of information between the site of data acquisition, the location of decision making and the location of final action being performed [5].

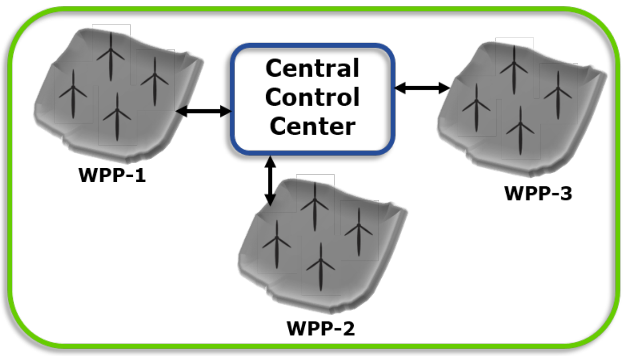

(a) Centralised Control

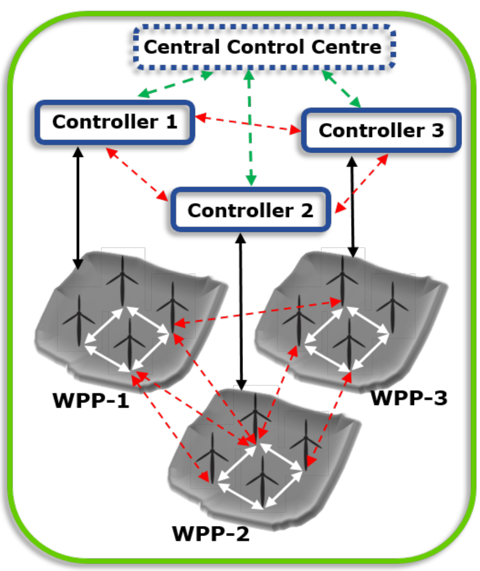

(b) Distributed control

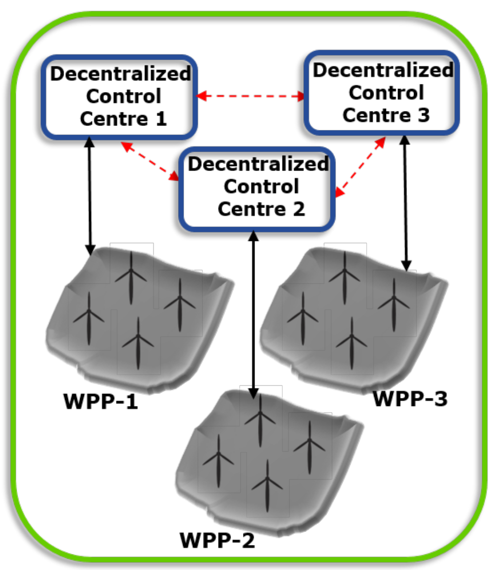

(c) Decentralized control

Figure 1: Conceptualisation of control architectures for a large OWPP cluster.

1.2 Centralized Control

A centralised control as illustrated in *Figure* 1(a) typically consists of a single control unit which prepares and sends power set points signals to each individual WT control [2], [6]. In a centralized control scheme, all the information available about the system, the calculations based upon this information, decision making and the enhancement of the decisions are all centralized i.e., concentrated in a single location. The control algorithms, the turbine controller, the WPP controller and the central controller receive information about the system from many sensors.

The feedback process helps to ensure that the system can adapt to different conditions, but also makes it vulnerable to loss or corruption and interruption of information which can have detrimental impact on the overall system. As it is responsible for the control of the entire WPP cluster, so it necessitates a fast powerful computer centralizing the control of the overall plant [3]. However large scale systems (WPP clusters) could be difficult to control with a centralised control structure due to required computational complexity, robustness and reliability problems as all the information flow is channelized to a single control unit and communication bandwidth limitations [7].

1.3 Distributed Control

The control problem could be broken down into manageable sub-problems such that the overall cluster is no longer controlled by a single controller, but several independent controllers locally such as decentralized structures and distributed control systems [7], [8]. In a distributed control scheme, multiple controllers work together with consensus, exchanging information with their neighbours to produce a desired power profile [9], [10]. It consists of a number of local controllers, each of which controls a subset of the system, with capability of communication between the controllers. The algorithms running in each agent take decisions with partial information about the system state provided by the other agents. The data may be processed locally or remote-controlled by a central controller as shown in *Figure* 1(*b*).

As large OWPPs network is spread over a large geographical area, having distributed control units also improves cybersecurity and resilience of the network with respect to failure of some parts of the network. For instance, in case any of the local controllers or components fail, it will affect only a small part of the network instead of the entire network. Additionally, it may also provide a certain degree of privacy since not all information is communicated. However, it also presents some challenges such as the proper design of a distributed algorithm, the reliability of the communication network and coordination of the agents to achieve the desired power regulation with limited information exchange. In the last few years, some encouraging progress has been reported in the area of distributed control [9], [7]. A two-step distributed Kalman filtering is proposed in [10]. In [11], a centralized controller paradigm is derived based on "model predictive control" in parallel with a distributed controller where the turbines essentially only communicate with their neighbours.

1.4 Decentralized Control

A decentralised control [12] shown in $Figure\ 1(c)$ is similar to a subset of a distributed control system, in that, every node is independent of each other. The control problem is partitioned into manageable sub-problems, each of which has a local independent controller [13] and the resulting behaviour is the aggregated response. However, the information could be shared between the local decentralized control centres to solve the larger problem. Many efforts have been devoted to develop design methods guaranteeing stability and performance of decentralized control. Among them are few based on Lyapunov functions [14], sequential design [15], optimization [16] and overlapping decompositions [17]. A decentralized coordinated voltage control scheme for VSC-HVDC connected OWPPs is proposed in [8] to regulate voltages within the feasible range by optimally coordinating the WPP side VSC and WTs based on Model Predictive Control (MPC). A novel decentralized control of offshore WPPs connected to onshore grid through a HVDC by means of a diode rectifier is proposed in [18].

2 System Configurations for DC Collection Systems and DC Wind Turbine Concept

Written by Gayan Abeynayake - Cardiff University, UK

2.1 Introduction

Currently, there are no operational offshore wind farms with DC collection grids, only theoretical and small-scale prototypes are being investigated. Therefore, a suitable configuration for the wind farm with DC collection grid which has been practically verified is not available yet [19]. The total power produced by the Wind-Energy Conversion Units (WECU) on the wind farm is collected, via an AC collection grid (traditionally), and transferred to onshore grid. Depending on the distance to the onshore grid and the power rating, either the HVAC or HVDC transmission system can be used for the power delivery. At present, most of the offshore wind farms are planned to be installed far from the shore, e.g. at a distance more than 60 km [20]. For tracking of maximum wind energy and for some other environmental issues such as to minimise the visual and audible impacts on nearby residences; the HVDC system is a preferable option than the HVAC system [21].

A typical configuration of an AC offshore wind farm with HVDC transmission system can be found in [22]. The power transformer station is installed on an offshore platform which steps up the voltage to 220 kV across the AC collector or AC bus. A short AC cable transfers power to the HVDC-rectifier platform, on which power converter is installed for HVAC to HVDC conversion. Once onshore, an HVDC-inverter platform is used for HVDC to HVAC conversion. A total of three platforms are required for an offshore wind farm integrating an AC collection grid with HVDC transmission line. The advantages of using HVDC transmission system is that low quantity of DC cables is needed, no charging current, and skin effect exist in the DC cables, power factor is always close to unity and there is less corona loss and radio interference.

For the design of a DC collection grid, the 50 Hz or 60 Hz power transformers installed in the WECUs are replaced by the power converters or rectifiers. The power converters are significantly compact and smaller in size compared with the power transformers of similar power rating. This reduces the size and weight of WECUs, and hence the offshore wind farm. For an offshore wind farm with DC collection grid and HVDC transmission system, a total of two platforms (rectifier and inverter stations) are needed, this also reduces the cost of platform installation. Technically, the power converters in WECUs perform power rectification, power conditioning, power filtering, and power compensation. The power rectification enables the conversion of signals (voltage and current) from AC to DC. The power conditioning provides the control of frequency, voltage, power factor, and speed of rotating machines. The power filtering injects (or absorbs) specific signal components for power quality.

2.2 Different DC Collection System Configurations

The DC collection grid for offshore wind farm begins with power converters at each WT, (usually in the base of the tower), which steps up the voltage output of the generator, typically 690 V, to a medium voltage of typically 25–40 kV. A medium-voltage submarine DC cable is used to connect the WECUs to a DC platform. Furthermore, the power converter performs the following functions:

1. Power Rectification to Convert Signals (Voltage and Current) from AC to DC

2. Power Conditioning to provide the control of voltage and speed of rotating machines

3. Power filtering to inject (or absorb) specific signals components for power quality

Typical configurations of the wind farm with DC collection systems are presented in Fig. 2. The WECUs are connected into multiple strings or several branches circuits that feed into an offshore platform. These configurations can be mainly classified in to two:

1. Shunt (or radial) Configurations

2. Series (or ring) Configurations

Other topologies proposed in the literature are improved/modified versions of the above two main topologies. Single-sided radial feeder and Bifurcated-radial feeder topologies belongs to shunt configuration. Single-sided ring feeder configuration and Double-sided ring feeder configuration can be identified as two different series configurations as discussed in [23].

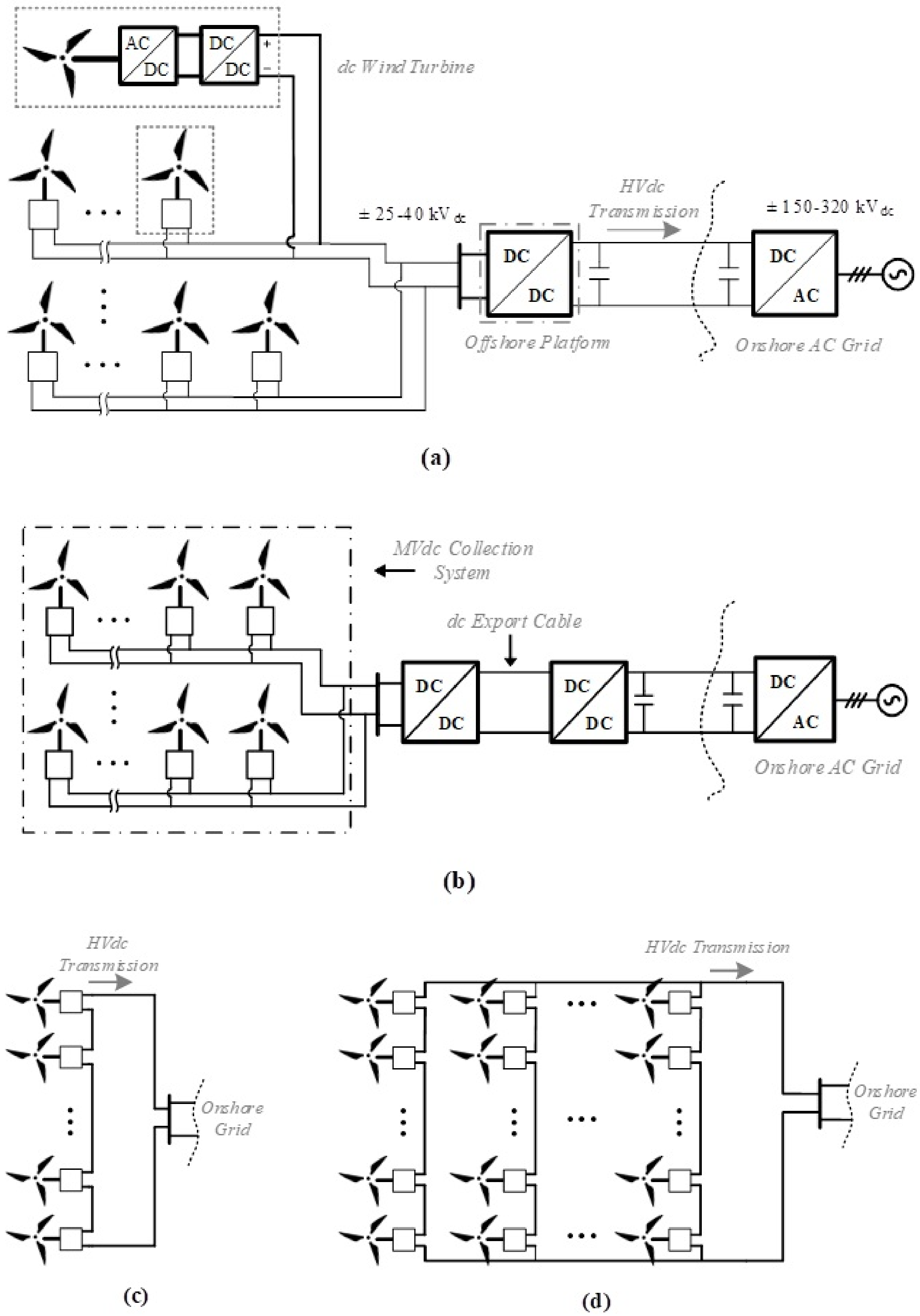

Figure 2: DC collection system configurations a) Shunt Configuration-1; b) Shunt Configuration-2; c) Series Configuration d) Series-Parallel Configuration

2.2.1 Shunt / Radial Configurations

Most of the wind farms today use the radial feeder configurations, because of low cable costs and simple control scheme. However, the drawback of the radial feeder configuration is poor reliability, since a cable fault at the hub end of the radial cluster may prevent the operation of the entire offshore power plant. The parallel connected WECUs on each string are exposed to same terminal voltage, which is the medium DC voltage. Each string can generate a total current $i_{dc}(t)$, given by equation 1, where $i_{do}(t)$ is the total current output of each WECU; and k represents the total number of WECUs on each string. A medium-voltage submarine DC cable is then used to connect the WECUs to an offshore platform. By considering n as the total number of strings on the wind farm; thus, the total current collected from the wind farm output can be obtained using equation 2.

$$i_{\mathrm{dc}}(t) = \sum_{k=1}^{k} i_{\mathrm{do(k)}}(t) \tag{1}$$

$$i_{\mathrm{DC}}(t) = \sum_{n=1}^{n} i_{\mathrm{dc(n)}}(t) \tag{2}$$

It can be observed that the use of HVDC-offshore platform is compulsory in order to step up the medium DC voltage to HVDC for transmission. The parallel-connected WECUs in each string increases (or builds up) the current magnitude according to equation 1, but the WECUs operate at identical terminal voltage magnitude. Consequently, an offshore platform is needed to step up the voltage to HVDC for transmission. Due to the fact that the output terminal of each WECU in the radial feeders is connected to a medium voltage link, (i.e. 25-40 kV) and also the voltage-boost ratio is high, (i.e. from 690 V to a medium-voltage level) all WECUs on a wind farm with radial feeder topology must integrate power converters with high boost ratio and that can support a medium-voltage level.

Actually, most of WECUs employed in the DC collection grids with radial feeders integrate 'the three-phase VSC cascaded with an isolated boost DC–DC converter which consists of an Single Active Bridge (SAB) or a Dual Active Bridge (DAB) DC-DC boost converter including a medium/or high frequency transformer', these power converter topologies have generally an HV-boost ratio, and also they are suitable for medium-voltage applications.

2.2.2 Series / Ring Configurations

The ring feeder configurations can provide higher reliability index than the radial feeder configurations. The drawback with the ring feeder configuration is that the series-connected converters must have the ability to operate toward a very HV. This is due to the fact that if one WECU fails, and therefore its terminal DC voltage collapses leading to loss of output power, the other WECUs must compensate for this by increasing their output voltage. For the ring feeder topology or Fig. 2 (c) and (d), the series connected WECUs in each string build up a voltage $V_{dc}(t)$ across the DC collector as given by equation 3, where $V_{do}(t)$ is the output voltage of each WECU; and k represents the total number of WECUs in the series-connected circuit.

$$V_{\mathrm{dc}}(t) = \sum_{k=1}^{k} V_{\mathrm{do(k)}}(t) \tag{3}$$

For this topology, the use of HVDC platform can be avoided; a voltage high enough for the HVDC transmission system can be achieved by increasing k, according to equation 3. The ring feeder configuration is the most simplified and cost-effective layout of offshore wind farm with DC collector systems; low-voltage-based converter topologies can be integrated in the WECUs. Other configuration options for offshore wind-power plants consist of multi-terminal HVDC systems connecting several wind farms. Among these configuration methods one can find [24], [25], [26]:

1. The radial connection where a group of interconnected wind farms is connected to a single HVDC platform; with this option, losing one pole in a bipolar HVDC transmission system may cause wind generation curtailment.

2. The split connection, where a single offshore wind farm is connected to a separate HVDC platform.

3. The backbone connection, and/or the grid connection; with several groups of wind farm where each group has a separate HVDC platform.

2.3 Main Components of a DC Collection System

Most of the traditional offshore wind farms are constructed with aggregation of WECUs. Each WECU comprises of a WT with mechanical parts, e.g. drive trains, a generator, e.g. Doubly Fed Induction Generator (DFIG), or Permanent Magnet Synchronous Generator (PMSG) including power electronics circuits, and a huge 50 Hz or 60 Hz power transformer. The large quantity of magnetic components employed in the power transformer makes the WECUs to be less compact and not strong enough to withstand the high-speed winds. Presently, the needed equipment for designing a high-power medium voltage DC system are not available. Irrespective of the topology used the following two components are required to realise a high-power Medium Volatge dc (MVdc) offshore wind collection system [27];

2.3.1 DC/DC Converter

The lack of adequate concept for transforming voltages in a high-power DC grid is one of the major obstacles against the realization of DC collection system. The development and design of an eligible concept, for a highly efficient and cost-effective DC/DC converter will therefore be essential. For safety and security reasons galvanic isolation is required for high-power DC collection system. This galvanic isolated DC/DC converter consist of an inverter at the input side, transforming the DC voltage into an AC signal of a certain frequency as shown in Fig. 3. In contrast to conventional Pulse Width Modulation (PWM) converters used in drives, a sinusoidal signal is not needed, because the converter is not connected to sensitive load or grid.

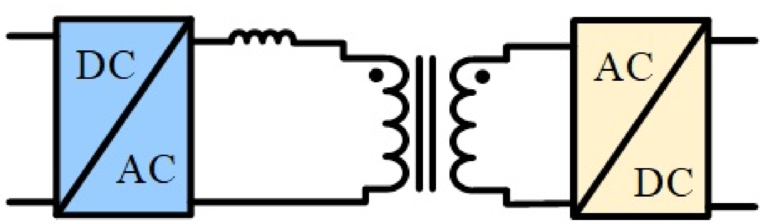

Figure 3: Configuration of an isolated DC/DC Converter

The considered converters can be separated into different groups using criteria like the possible directions of the power flow and whether soft-switching is applied or not as illustrated in Fig. 4. At first level, the converters are differentiated in resonant and hard/soft-switching converters. In the latter, all converters are consolidated without any additional devices which operate either under hard-switching conditions or can achieve soft-switching via proper control or design of the circuit. Unlike these solutions, the resonant converters are using additional passive components to achieve soft switching and reduce switching losses significantly. The term soft switching is used when the switching of the device occurs at a zero current or voltage crossing.

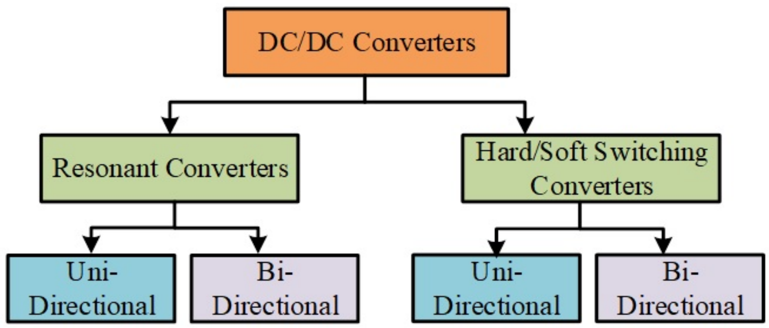

Figure 4: Different groups of isolated DC/DC Converter

2.3.2 DC Circuit Breaker

One major requirement of a high-power DCCB is a fast turning-off time, because otherwise the whole system must be designed for extremely high fault currents. In present AC systems a fast turn-off time is not crucial, because of the limiting grid inductance, but in a DC system the amplitude of the short-circuit current would in theory be 10 times higher than the amplitude in a similar AC system within 300 ms fault duration [27]. Two main requirements of a high power DC circuit breaker are

1. Ability to act quite rapidly to avoid extremely high currents and allow an active turn-off process
2. High voltage blocking capability during switching for the demagnetization of grid inductance

As discussed in [28], even though fault currents may be interrupted by certain converter topologies, a circuit-breaker capable of interrupting nominal currents becomes mandatory in order to disconnect lines without having to power down the entire grid. Until now, different concepts for the realization of DC circuit-breakers have been proposed in the literature following DCCBs can be significantly distinguished.

1. *Mechanical Breakers with High Arcing Voltages*

   This technology is available on commercial scale for railway systems. When the DC breaker is tripped, a mechanical contact opens and an electrical arc ignites. This arc is then moved into a stack of metal plates, which lead to a significant increase of the arcing voltage. For discharging the line inductances and decreasing the current, the voltage across the arc must be higher than the nominal grid voltage. As soon as the current is zero, the arc extinguishes and the fault is cleared.

2. *Solid-State DC Circuit Breakers*

   Compared to present circuit breakers, Solid-State DC Circuit Breakers (SSCB) have the advantage of interrupting the current before the maximum amplitude is reached, resulting in reduced current amplitudes and short voltage disturbances. However, SSCBs are expensive and high losses due to semiconductor conduction losses. A simple topology of a SSCB is shown in Fig. 5.

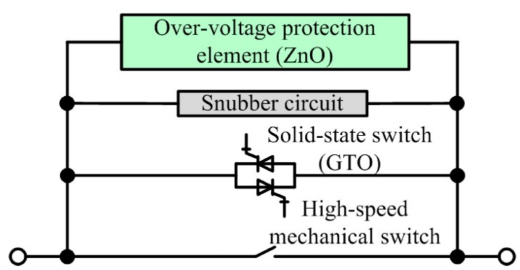

Figure 5: Solid-State DC Circuit Breaker Topology

   When the DC breaker is tripped, the GTO is turned off. Due to the inductively stored energy, the voltage across the semiconductors rises quickly and the surge arrester starts conducting current. In order to discharge the line inductance, the protection voltage of the surge arrester must be higher than the nominal grid voltage. Also, it must be ensured that the power semiconductors are able to withstand the protection voltage of the surge arrester. The main advantage of a solid-state DC breaker is its fast interruption speed and the lack of moving parts.

3. *Hybrid DC Breakers*

   Hybrid DC Breakers combine a mechanical switch and a solid-state breaker to overcome the disadvantage of high on-state losses and the lack of DC current interruption capabilities of mechanical switches [29]. The layout of the conventional hybrid DC breaker is shown in Fig. 6. The interruption process is similar to the solid-state breaker. However, before the power semiconductors, in this case Insulated Gate Bi-polar Transistor (IGBT)s are used, can interrupt the fault current, the mechanical switch must be open and the fault current has to commutate into the parallel power semiconductors. Since the opening of the mechanical switch and the commutation process require some time, the overall interruption process is slower in comparison to the solid-state breaker.

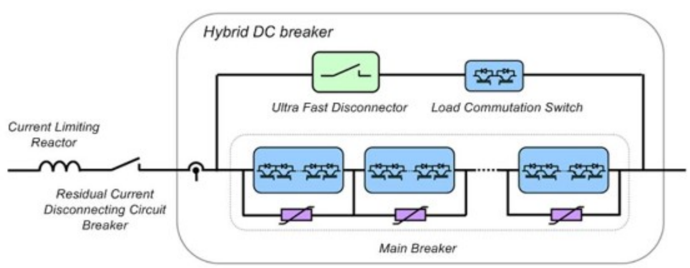

Figure 6: Hybrid DC circuit Breaker Topology

2.4 The DC Wind Turbine Concept

There are several dcWT concepts discussed in the literature as illustrated in Fig. 7. They are classified according to the number of converter stages assuming state-of-the-art wind generators are employed [30].

The first concept (Fig. 7(a)), employing only 1 stage, that of an active rectifier and has the advantage of low number of components and simplicity. The problem is that maximum output voltage is limited to the generator's nominal voltage level and it has no galvanic separation. Therefore, concept from Fig. 7(b) could alleviate this issue, by simply adding non-isolated dc/dc converter, to step up to medium voltage level. Another 2-stage concept ((Fig. 7(c) suggests a low frequency transformer followed by a passive rectifier. Simplicity and low number of components are advantages, but fixed speed operation and transformer saturation risks are main disadvantages. Another interesting concept composed of 3 stages (Fig. 7(d)) was proposed by [31] and employs a matrix converter (AC/AC).

Further on, a 4-stage concept (Fig.7(e)) that reuses the AC turbine's generator and active rectifier, followed by an isolated high-power dc/dc converter. This approach would imply that the main research focus should be on the DC/DC converter, while the rest of components are off the shelf and present low technology risk. It also presents the lowest impact on AC turbine design to turn it into DC turbine. For these reasons it will be the main framework of this research. A final turbine concept, with 5 converter stages (Fig. 7(f)) incorporates a boost converter between the active rectifier and the isolated DC/DC converter. The topology was suggested in [32], and it assumes that the boost converter is actively controlling the LV side DC link, while the DC/DC converter is operated in open loop in the manner of a DC/DC transformer.

2.4.1 Selection of a suitable DC/DC Converter

The DC/DC converter shall consider as a combination of power conversion stages 2,3 and 4 of Fig. 7(e). This DC/DC converter topology could be SAB or DAB which operates on phase-shift control principle. In wind power applications the active power flow is always unidirectional i.e. from WT side to grid side. Therefore, SAB will primarily serve our requirement. However, the major limitation of SAB is phase shift between primary and secondary occurs due to the leakage inductance of the medium frequency transformer

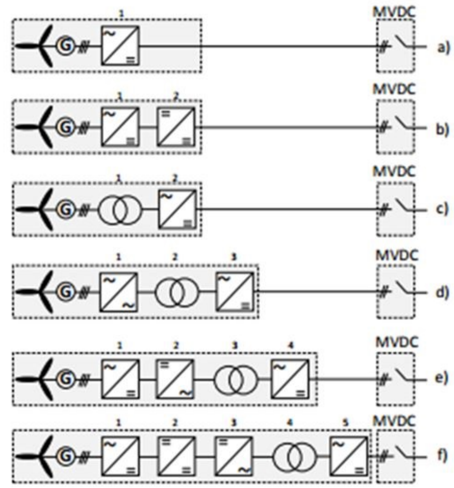

Figure 7: dcWT Concepts [30]

[33]. Thus, to transfer large amount of power transformer leakage inductance should made very low. This problem shall eliminate with the use of DAB.

Generally, DAB is used when bi-directional power transfer is required such as in dc microgrids. However, DAB shall support for OWPP black-start by enabling reverse power flow to charge the dc-link of the dcWT. If SAB is used, there should be a stand-by diesel generator ready at all times. With severer marine weather conditions re-fuelling of diesel generators could be problematic. Thus, use of DAB as the DC/DC converter in topology-(e) is advantageous. In general, converter reliability is also an important aspect to be considered as discussed in [34].

2.4.2 Control Modes of DC Wind Turbine

As shown in Fig. 8. the main control objectives of topology-(e) (refer together with Fig. 7(e)) are dc link voltage control and active power control. This is similar to control of PMSG based full-scale acWT with interchange of control responsibilities. The dc link voltage is controlled by Voltage Source Converter (VSC) connected to wind generator and power is regulated by DAB on phase-shift control mode.

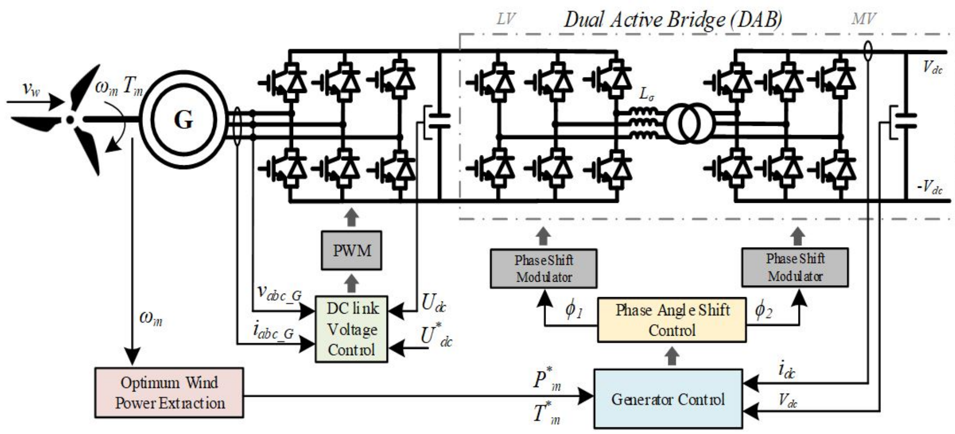

Figure 8: Control scheme of dcWT topology-(e)

1. DC link Voltage Control

   The Grid Side Converter (GSC) is responsible for maintaining the DC link voltage constant and it is able to provide reactive power. Typically, the control objective is achieved by the vector control which is based on dq components. This consists of an outer loop that regulates the DC voltage through a PI controller and an inner loop that controls the current.

2. Generator Control

   The Rotor Side Converter (RSC) controls the power extracted from the wind turbine or the mechanical torque. However, in [35] it has shown that it is possible to swap control objectives of GSC and RSC with enhanced fault ride-through and voltage support capabilities.

3 Economic Analysis of different Transmission Options

Written by Jovana Dakic - UPC, Spain

3.1 System Description

3.1.1 High Voltage Alternating Current Systems

The High Voltage Alternating Current (HVAC) power transmission system is based on two substations connected with cross-linked polyethylene (Cross Linked Polyethylene (XLPE)) cables. The substations include power transformers, gas or air insulated switchgears and reactive power compensation equipment. Today, XLPE cables are the most used submarine cable technologies for HVAC transmission systems. They can be either single-core or three-core, but three-core cables have the advantage due to reduced power losses and less installation costs [36]. The collector grid operates in the range of 33-66kV, so the voltage is stepped up to the offshore transmission level with an offshore transformer. If the onshore grid operating level differs from the transmission one, an onshore transformer is also needed. In order to increase the power export availability of the substations, the preferred transformer topology is installing two transformers in parallel, rated at 60 % of the offshore wind farm nominal power [37].

The reactive power generated in the cables increases with the cable length and therefore limits the active power that will be delivered to the grid and the cable length of the offshore transmission link. [38]. Reactive power compensation leads to reduction of power losses and voltage control. Fixed compensation could be installed at different locations along the cable and static synchronous compensator (Static Synchronous Compensator (STATCOM)) is usually located at the onshore substation to meet the grid requirements [39]. Fig. 9 illustrates a system diagram of a HVAC offshore transmission system.

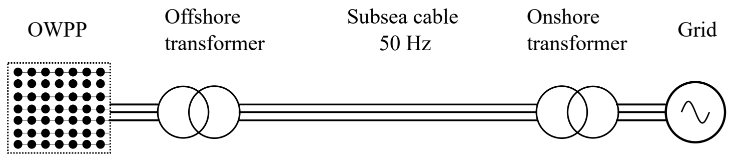

Figure 9: Basic configuration of HVAC solution

3.1.2 High Voltage Direct Current Systems

There are two converter technologies used for High Voltage Direct Current (HVDC) transmission systems for offshore wind: line commutated converters ((Line Commutated Converter (LCC))) and voltage source converters ((VSC)). However, due to the big number of commutation failures and no black start capability of LCCs, today VSC based transmission systems are recognized as a more suitable solution for OWPPs. HVDCVSC is constructed from two system elements, including two converter stations (one offshore and one on shore) and a pair of polymeric extruded cables. The technology is based on IGBT semi-conductors, which results in low number of harmonics in the system due to the switching frequency (1.3-2.0kHz). The use of advanced PWM technology enables bidirectional power transmission [40] Furthermore, in VSCs the control of the active and the reactive power is done independently, which leads to voltage and frequency stability [41]. Fig. 10 shows a basic HVDCVSC system configuration for offshore wind farms.

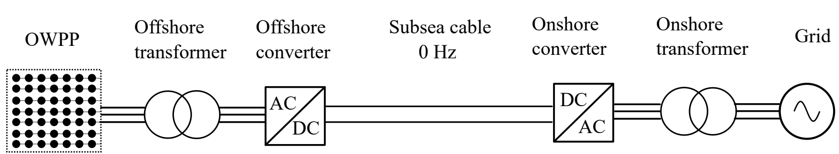

Figure 10: Basic configuration of HVDC solution

3.1.3 Low Frequency Alternating Current Systems

Low-frequency alternating current (LFAC) is a new suggested technology combining the HVDC and HVAC system in order to eliminate their technical disadvantages. LFAC systems work at a smaller frequency (usually one-third of the grid frequency value). With lower frequency, charging current is still present, but in a smaller value. The contribution is seen in less costs related to reactive power compensation and increased amount of transmitted power. Additionally, as Alternating Current (AC) resistance of the cables is dependent of proximity and skin effects, with lower frequency, ohmic power losses are reduced [42]. Fig. 11 shows the system diagram of a LFAC system. The configuration proposes that the wind power plants generates power at low frequency. The latter implies that both the collection system and the power transmission is made at 50/3 Hz, excluding a frequency conversion in the offshore substation [43]. The proposals of the technology of the onshore frequency converter are Cycloconverter or Back-to-Back (Back to Back (B2B)) technology [44]. The main drawback is the size of transformers, as low frequency requires larger transformers, which also leads to bigger offshore substations [45, 46].

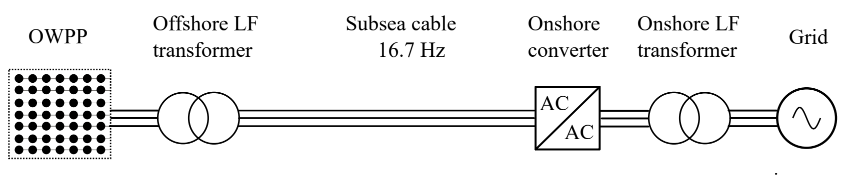

Figure 11: Basic configuration of LFAC solution

3.2 Cost Modelling

This section gives a description of cost models for HVAC, HVDC and LFAC. The capital investment costs, as well as modelling of losses and its cost are presented separately for each component.

3.2.1 HVAC Cost

3.2.1.1 Common System Variables The chosen frequency f_{HVAC} is 50Hz, but other values could be introduced (60Hz), depending on the location of the power plant.

The standardized voltage levels $U_{rms,HVAC}$ for subsea transmission is in range of 110-400 kV [47]. The rated current of the cable (ampacity) $I_{rated,HVAC}$ is chosen from the supplier's catalogue [47] based on the calculated current passing through the cables:

$$I = \frac{k \cdot P_{owf}}{\sqrt{3} \cdot U_{rms,HVAC}} \tag{4}$$

where k is the coefficient for current tolerance of $+10\%$ ($k = 1.1$) and P_{owf} is the rated power of wind power plant. Later, the correspondent three-core cable conductor cross-section S_{HVAC} is taken following the catalogue. Finally, the number of three-core cables $n_{cb,HVAC}$ should be chosen.

3.2.1.2 Cable As cable technology is developing rapidly, cost modelling has become challenging to include all factors effecting the total cost. Lundberg first modelled the cost of three core cable modelled through an exponential equation with an offset constant [48]. The two most important factors affecting the cost are: rated current of the cable (relates to the amount of copper (or aluminum) used in the cable) and the rated voltage of the cable (determines the insulation material). In [49], the equation is updated with the influence of the cable installation which is considered as the highest uncertain factor. Cost of cable C_{cb} is presented:

$$C_{cb} = \frac{(A + Be^{CS_{rated,HVAC}} + D) \cdot (9n_{cb,HVAC} + 1)}{10E} \cdot l \tag{5}$$

where the constant values (A, B, C, D, E) are defined in Table 1, which are dependent on the cable voltage [48, 50] and l is the transmission distance. $S_{rated,HVAC}$ is the rated apparent power of the cable in [MW]:

$$S_{rated,HVAC} = \sqrt{3} \cdot U_{rms,HVAC} \cdot I_{rated,HVAC} \tag{6}$$

Table 1: Coefficients for XLPE submarine AC cables [48, 50]

	30 kV	70 kV	150 kV	220 kV	400 kV
A	0.411	0.688	1.971	3.181	5.8038
B	0.596	0.625	0.209	0.11	0.044525
C	0.041	0.0166	0.0166	0.0116	0.0072
D			$17 \cdot 10^4$		
E			8.98		

3.2.1.3 Switchgear

The avaliable data is in [51]. With interpolation method, the cost of a switchgear can be obtained:

$$C_{gis} = 0.0117 \cdot U_{rms,HVAC} + 0.0231 \tag{7}$$

The switchgear is needed at the sending and receiving point of the offshore and onshore substation as its function is protection between critical components. Therefore, the number of necessary High Voltage (HV) switchgears will be two per cable.

3.2.1.4 Transformer

Cost of transformer is dependent of its rated power S_{TR} [MVA] and assumed based on [52]

$$C_{TR} = 0.0427 \cdot S_{TR}^{0.7513} \tag{8}$$

As discussed in 3.1.1, the number of the transformers will be four, two at each substation with rated power $S_{TR} = 0.6 \cdot P_{owf}$.

3.2.1.5 Substation

The cost of offshore substation platform depends on its volume. The electrical infrastructures and the presence of additional services (e.g. living quarters, heliport, and fuel tanks) define the volume. The cost for such a substation can be expressed by the following equation [53, 48]:

$$C_{ss} = 2.534 + 0.0887 \cdot P_{owf} \tag{9}$$

where P_{owf} is the rated power of the offshore wind power plant [MW].

3.2.1.6 Reactive Power Compensation

Regarding to fixed compensation, the cost is related to its location and reactive power absorbed by the compensation. The linear equation is derived from [51, 54, 38, 55]:

$$C_{react} = K \cdot Q_l + P \tag{10}$$

The constant values (K, P) are defined in Table 2 and Q_l is the compensated reactive power.

For a 100-MVAr and a 200-MVAr STATCOM, the reported costs are, respectively, in the range of 5,75 to 11,5 M€ and 11,5 to 23 M€ [51], giving an approximate cost of 0.086 M€/MVAr.

Table 2: Coefficients for fixed compensation

Location	K	P
Onshore	4.2	0.8283
Offshore	6.096	1.279
Middle	18.096	1.543

3.2.1.7 Power Losses The cost of power losses C_{loss} is presented:

$$C_{loss} = 8760 \cdot c_{owf} \cdot t_{owf} \cdot C_{energy} \cdot P_{loss} \tag{11}$$

where c_{owf} is the capacity factor of the wind power plant, t_{owf} is the life time of the wind power plant in years, C_{energy} is the cost of energy in €/MWh.

The power losses in the system P_{loss} are expressed as ohmic losses, i.e. $\sum R_i I_i^2$ where R_i is the equivalent resistance of element i and I_i is the current through that element. Losses from all elements are considered as follows:

$$P_{loss} = P_{loss}^{onTR} + P_{loss}^{cb} + P_{loss}^{offTR} \quad [MW] \tag{12}$$

where is P_{loss}^{onTR} are losses of onshore transformers, P_{loss}^{cb} are losses of the cable and P_{loss}^{offTR} are losses of offshore transformers.

3.2.2 HVDC Cost

3.2.2.1 Base variables In order to obtain the costs for a HVDC transmission system, a set of variables are introduced. The voltage levels U_{HVDC} are in range from ±80-320 kV. The number of cables pairs $n_{cb,HVDC}$ is by default usually equal to 1 as the system is bipolar. Each cross section S_{HVDC} and cable rated current $I_{rated,HVDC}$ is estimated from the values given by suppliers.

3.2.2.2 Cable Including investment and installation cost in one equation, cost of cable $C_{cb,HVDC}$ is presented in [49]:

$$C_{cb,HVDC} = \frac{(A + BP_{rated,HVDC} + D) \cdot (9n_{cb,HVDC} + 1)}{10E} \cdot l \tag{13}$$

where the constant values (A, B, D, E) are defined in Table 3 which are dependent on the cable voltage and l is the transmission distance [km]. The rated power of cable pair is calculated as following:

$$P_{rated,HVDC} = 2 \cdot U_{HVDC} \cdot I_{rated,HVDC} \tag{14}$$

Table 3: Coefficients for Direct Current (DC) cables [48, 50]

Voltage levels	±80 kV	±150 kV	±220 kV
A	$-0.25179 \cdot 10^6$	$-0.1 \cdot 10^6$	$0.286 \cdot 10^6$
B	0.03198	0.0164	0.00969
D		$22 \cdot 10^4$	
E		8.98	

3.2.2.3 Transformer HVDC systems also need transformers to step up the voltage from the collection grid to the transmission cables and further on to the grid. The same optimal configuration with two transformers at each substation is assumed and cost function shown in 8 is used.

3.2.2.4 Substation Due to the IGBT-based AC/DC converters, the substation cost is higher for the HVDC option. Additional elements are needed: power electronics, phase reactors, filters, transformers, enclosed valves, etc. From data in [51], it is evaluated that a HVDC substation costs are from 57,9% to 115,4% higher than a HVAC one for the same rated power. An average number of 85% is taken in account and the cost function is obtained:

$$C_{ss} = 1.85 \cdot (2.534 + 0.0887 \cdot P_{owf}) \tag{15}$$

where P_{owf} is the rated power of the offshore wind power plant [MW].

3.2.2.5 HVDC Converter Station The difference between offshore and onshore converter stations is quite significant because of offshore installation.The VSC converter offshore and onshore are defined in the following equations [49, 52, 50]:

$$C_{dc,off} = 42 + 27 \cdot \frac{P_{N,conv}}{300} \tag{16}$$

$$C_{dc,on} = 18 + 27 \cdot \frac{P_{N,conv}}{300} \tag{17}$$

where $P_{N,conv}$ is the rated power of the converter.

3.2.2.6 HVDC Converter Losses Regarding the losses in the converter, several approaches have been found.The switching and conduction losses $P_{loss,conv}$ of a VSC could be estimated by a quadratic polynomial function considering three parts: constant, linear and quadratic losses. It is determined by the converter current I_c [56]:

$$P_{loss}^{conv} = [a + b \cdot \frac{I_c}{I_r} + c \cdot (\frac{I_c}{I_r})^2] \cdot S_n \tag{18}$$

where I_r is the rated converter current, S_n represents the nominal apparent power. Typical loss data for a two level VSC HVDC can be found in [57]. For the modular multilevel (Modular Multi-Level Converter (MMC)) topologies based on "Half-Bridge" valves result in total losses per converter station of approximately 1% per end [58]. The cost of VSC converter losses is evaluated as:

$$C_{loss,VSC} = P_{loss,VSC} \cdot 8760 c_{owf} \cdot t_{owf} \cdot C_{energy} \tag{19}$$

where it is assumed that the VSC losses are 1% of the converted power, obtaining the following equation:

$$P_{loss,VSC} = 0.1 \cdot c_{owf} \cdot P_{owf} \tag{20}$$

The equations for the cost of power losses remain the same as in Section 3.2.1.7.

3.2.3 LFAC Cost

LFAC transmission systems have not been yet implemented in industry, so only theoretical cost comparison has been done in [54], whereas the cost of some components at non-standard frequencies is estimated in [45] .

The components that are most affected by low frequency is the transformers, especially the capital cost because of its volume increase. Consequently, the substation platform would have changes in the cost. The costs of the necessary AC-AC frequency converter (Cycloconverter or B2B-VSC) is also analysed. For the other components of the system, the same cost functions as for HVAC systems will be used.

3.2.3.1 Common System Variables The electric line frequency f_{LFAC} is 16,67Hz (standardized value for railway), but other values could be introduced.

The standardized voltage levels $U_{rms,LFAC}$ for subsea transmission are same as for HVAC. The rated current of the cable (ampacity) $I_{rated,LFAC}$ and following cross-section S_{LFAC} is chosen. Therefore, the number of three-core cables $n_{cb,LFAC}$ are determined.

3.2.3.2 Transformer The total cost of the transformer can be calculated depending on the frequency [45]:

$$C_{TR,LFAC} = \frac{0.325 f_r + 0.22 f_r + 0.164 \sqrt[3]{f_r^2}}{0.325 + 0.22 + 0.164} \cdot C_{TR} \qquad (21)$$

where f_r is the normalized frequency, calculated $f_r = \frac{f_{HVAC}}{f_{LFAC}}$.

3.2.3.3 Substation The platform size is affected due to the transformer size, therefore the cost as well. The cost function is derived from [53]:

$$C_{ss} = (2.534 + 0.0887 \cdot P_{owf}) \cdot (\frac{1}{3} + \frac{2}{3} f_r) \qquad (22)$$

3.2.3.4 Frequency Converter As mentioned in 3.1.3 there are two possibilities of frequency converters. In previous research [59, 60] it is considered that Cycloconverter technology may have lower losses and costs than IGBT solution. On the other hand, as Cycloconverter is thyristor based, high number of harmonic is present, so large number of filter are needed which affects the size of substation. Furthermore, it requires reactive power compensation as the technology does not have independent control of reactive power. Due to this drawbacks, theB2B-VSC based converter is suggestion as a more optimal solution. B2B-VSC includes an independent control of active and reactive power, black start capability and no filtering [44].

B2B converter costs are found to be €143/kVA [61, 62]. A Siemens report comparing Cycloconverters and VSCs for the application of grinding mills (converters rated at 32 MW) states that the cost of a VSC is 140% the cost of a Cycloconverter [61] which leads to approximately €105/kVA. Both Cycloconverter and B2B-VSC converter should be considered to verify if less costs of cycloconverter compensate the the technical disadvantages compared to the B2B-VSC converter. The losses of the converters are assumed same as the -VSC one (1% of the converted power) so the same cost function (Equation (19)) will be used.

References

[1] Jesper R Kristoffersen and Peter Christiansen. Horns rev offshore windfarm: its main controller and remote control system. *Wind Engineering*, 27(5):351–359, 2003.

[2] Anca D Hansen, Poul Sørensen, Florin Iov, and Frede Blaabjerg. Centralised power control of wind farm with doubly fed induction generators. *Renewable energy*, 31(7):935–951, 2006.

[3] Alejandro. J Gesino. Power reserve provision with wind farms. *PhD thesis*.

[4] A Gesino, C Quintero, R Mackensen, M Wolff, B Lange, and K Rohrig. Wind farm cluster management system. In *XV Energie Symposium, Fachhochschule Stralsund, Nov 6th–Nov. 11th*, 2008.

[5] Shahab Asadollash, Rongwu Zhu, and Marco Liserre. Analysis of voltage control strategies for wind farms. *IEEE Transactions on Sustainable Energy*, 2019.

[6] Anca D Hansen, Poul Sørensen, Florin Iov, and Frede Blaabjerg. Grid support of a wind farm with active stall wind turbines and ac grid connection. *Wind Energy*, 9(4):341–359, 2006.

[7] Riccardo Scattolini. Architectures for distributed and hierarchical model predictive control–a review. *Journal of process control*, 19(5):723–731, 2009.

[8] Yifei Guo, Houlei Gao, Hao Xing, Qiuwei Wu, and Zhongwei Lin. Decentralized coordinated voltage control for vsc-hvdc connected wind farms based on admm. *IEEE Transactions on Sustainable Energy*, 10(2):800–810, 2018.

[9] Bassam Bamieh and Petros G Voulgaris. A convex characterization of distributed control problems in spatially invariant systems with communication constraints. *Systems & control letters*, 54(6):575–583, 2005.

[10] Peter Alriksson and Anders Rantzer. Distributed kalman filtering using weighted averaging. In *Proceedings of the 17th International Symposium*

on Mathematical Theory of Networks and Systems, pages 2445–2450. Kyoto Kyoto, Japan, 2006.

[11] Torben Knudsen, Thomas Bak, and Mohsen Soltani. Distributed control of large-scale offshore wind farms. In *European Wind Energy Conference and Exhibition (EWEC) 2009*. European Wind Energy Association (EWEA) Parc Chanot, Marseille, France, 2009.

[12] Lubomir Bakule. Decentralized control: An overview. *Annual reviews in control*, 32(1):87–98, 2008.

[13] Edward J Davison and Timothy N Chang. Decentralized stabilization and pole assignment for general proper systems. *IEEE Transactions on Automatic Control*, 35(6):652–664, 1990.

[14] Dragoslav D Siljak. *Decentralized control of complex systems*. Courier Corporation, 2011.

[15] Morten Hovd and Sigurd Skogestad. Sequential design of decentralized controllers. *Automatica*, 30(10):1601–1607, 1994.

[16] Riccardo Scattolini and N Schiavoni. A parameter optimization approach to the design of structurally constrained regulators for discrete-time systems. *International Journal of Control*, 42(1):177–192, 1985.

[17] M Ikeda, DD Šiljak, and DE White. Decentralized control with overlapping information sets. *Journal of optimization theory and Applications*, 34(2):279–310, 1981.

[18] Miguel Angel Cardiel-Alvarez, Santiago Arnaltes, Jose Luis Rodriguez-Amenedo, and Ashkan Nami. Decentralized control of offshore wind farms connected to diode-based hvdc links. *IEEE Transactions on Energy Conversion*, 33(3):1233–1241, 2018.

[19] D Berenguel, Mikel Gil, Oriol Bellmunt, and M Martins. Electrical interconnection options analysis for offshore wind farms. *European Wind Energy Conference and Exhibition, EWEC 2013*, 3:1759–1764, 01 2013.

[20] Mikel De Prada Gil, J.L. Domínguez-García, F. Díaz-González, M. Aragüés-Peñalba, and Oriol Gomis-Bellmunt. Feasibility analysis of offshore wind power plants with dc collection grid. *Renewable Energy*, 78:467 – 477, 2015.

[21] Lazaros P. Lazaridis and Jovan Todorovic Nicola Barberis Negra. Economic comparison of hvac and hvdc solutions for large offshore wind farms under special consideration of reliability, 2005.

[22] C. Chou, Y. Wu, G. Han, and C. Lee. Comparative evaluation of the hvdc and hvac links integrated in a large offshore wind farm—an actual case study in taiwan. *IEEE Transactions on Industry Applications*, 48(5):1639–1648, Sep. 2012.

[23] John Daniel, Shu Liu, Eduardo Ibanez, Ken Pennock, Gregory Reed, and Steve Hanes. National offshore wind energy grid interconnection study: Executive summary, 01 2014.

[24] G. Shi, Z. Chen, and X. Cai. Overview of multi-terminal vsc hvdc transmission for large offshore wind farms. In *2011 International Conference on Advanced Power System Automation and Protection*, volume 2, pages 1324–1329, Oct 2011.

[25] J. Yang, J. E. Fletcher, J. O'Reilly, G. P. Adam, and S. Fan. Protection scheme design for meshed vsc-hvdc transmission systems of large-scale wind farms. In *9th IET International Conference on AC and DC Power Transmission (ACDC 2010)*, pages 1–5, Oct 2010.

[26] Padmavathi Lakshmanan, Jun Liang, and Nicholas Jenkins. Assessment of collection systems for hvdc connected offshore wind farms. *Electric Power Systems Research*, 129:75–82, 12 2015.

[27] C. Meyer. *Key Components for Future Offshore DC Grids*. PhD thesis, 2007.

[28] M. Heidemann, G. Nikolic, A. Schnettler, A. Qawasmi, N. Soltau, and R. W. De Donker. Circuit-breakers for medium-voltage dc grids. In *2016 IEEE PES Transmission Distribution Conference and Exposition-Latin America (PES T D-LA)*, pages 1–6, Sep. 2016.

[29] Magnus Callavik, Anders Blomberg, Jürgen Häfner, and Bjoern Jacobson. The hybrid hvdc breaker an innovation breakthrough enabling reliable hvdc grids. 2012.

[30] Catalin Gabriel Dincan. *High power medium voltage DC/DC converter technology for DC wind turbines*. PhD thesis, 2018.

[31] R. Barrera-Cardenas and M. Molinas. Comparative study of wind turbine power converters based on medium-frequency ac-link for offshore dc-grids. *IEEE Journal of Emerging and Selected Topics in Power Electronics*, 3(2):525–541, June 2015.

[32] C. Schacherer M. Hergt, D. Kurthakoti. Connecting power plants to high voltage networks, U.S. Patent U2 2016/0149509A1, 2016.

[33] Max L. *Design and control of a dc collection grid for a wind farm*. PhD thesis, 2009.

[34] G. Abeynayake, G. Li, T. Joseph, W. Ming, and J. Liang. Reliability evaluation of voltage source converters for mvdc applications. *2019 IEEE Innovative Smart Grid Technologies - Asia (ISGT-Asia)*, pages 1–5, May 2019.

[35] A. D. Hansen and G. Michalke. Multi-pole permanent magnet synchronous generator wind turbines' grid support capability in uninterrupted operation during grid faults. *IET Renewable Power Generation*, 3(3):333–348, Sep. 2009.

[36] Van Hertem, Dirk, Gomis-Bellmunt, Oriol, and Jun Liang. HVDC grids: for offshore and supergrid of the future. *Wiley*, page 528, 2016.

[37] Andrew R Henderson, Lyndon Greedy, Fabio Spinato, and Colin A Morgan. Optimising Redundancy of Offshore Electrical Infrastructure Assets by Assessment of Overall Economic Cost. *European Offshore Wind Energy Conference*, (September 2009):14–16, 2009.

[38] Zhang Chen, Dui Xiaowei, and Zhu Guiping. Optimisation of reactive power compensation of HVAC cable in off-shore wind power plant. *IET Renewable Power Generation*, 9(7):857–863, 2015.

[39] A. Madariaga, J. L. Martín, I. Zamora, I. Martínez De Alegría, and S. Ceballos. Technological trends in electric topologies for offshore wind power plants. *Renewable and Sustainable Energy Reviews*, 24:32–44, 2013.

[40] Ervin Spahić and Gerd Balzer. Offshore wind farms - VSC-based HVDC connection. *2005 IEEE Russia Power Tech, PowerTech*, pages 1–6, 2005.

[41] Olof Heyman and ABB. HVDC Light ® It's time to connect. *ABB ID No. POW-0038*, pages 1–72, 2012.

[42] H. Chen, M.H. Johnson, and D.C. Aliprantis. Low-frequency ac transmission for offshore wind power. *IEEE Transactions on Power Delivery*, 28(4):2236–2244, 2013.

[43] P. B. Wyllie, Y. Tang, L. Ran, T. Yang, and J. Yu. Low frequency AC transmission-elements of a design for wind farm connection. *IET Seminar Digest*, 2015(CP654):1–5, 2015.

[44] Jonathan Ruddy, Ronan Meere, and Terence O'Donnell. Low Frequency AC transmission for offshore wind power: A review. *Renewable and Sustainable Energy Reviews*, 56:75–86, 2016.

[45] José Luis Domínguez-García, Daniel J. Rogers, Carlos E. Ugalde-Loo, Jun Liang, and Oriol Gomis-Bellmunt. Effect of non-standard operating frequencies on the economic cost of offshore AC networks. *Renewable Energy*, 44:267–280, 2012.

[46] Shenquan Liu, Xifan Wang, Lianhui Ning, Biyang Wang, Ming Lu, and Chengcheng Shao. Integrating Offshore Wind Power Via Fractional Frequency Transmission System. *IEEE Transactions on Power Delivery*, 32(3):1253–1261, 2017.

[47] X ABB. Submarine Cable Systems: Attachment to XLPE Land Cable Systems-Users Guide. 2011.

[48] Stefan Lundberg. Performance comparison of wind park configurations. *Power Engineering*, 2003.

[49] Hakan Ergun, Student Member, Dirk Van Hertem, Senior Member, and Ronnie Belmans. Transmission System Topology Optimization for Large-Scale Offshore Wind Integration HE European Union has set ambitious goals regarding. *IEEE Transactions on Sustainable Energy*, 3(4):908–917, 2012.

[50] B. Van Eeckhout, D. Van Hertem, M. Reza, K. Srivastava, and R. Belmans. Economic comparison of VSC HVDC and HVAC as transmission system for a 300MW offshore wind farm. *European Transactions on Electrical Power*, 20(5):661–671, 2010.

[51] ENTSO-E AISBL. Offshore Transmission Technology. *Entso-e*, pages 1–44, 2011.

[52] Lazaros P Lazaridis. Economic Comparison of HVAC and HVDC Solutions for Large Offshore Wind Farms under Special Consideration of Reliability. *Electrical Engineering*, 12(4):203–208, 2005.

[53] M. Dicorato, G. Forte, M. Pisani, and M. Trovato. Guidelines for assessment of investment cost for offshore wind generation. *Renewable Energy*, 36(8):2043–2051, 2011.

[54] X. Xiang, M. M. C. Merlin, and T. C. Green. Cost Analysis and Comparison of HVAC , LFAC and HVDC for Offshore Wind Power Connection. *IET 12th International Conference on AC andDC Transmission*, pages 14–19, 2016.

[55] Yongan Deng. 1 . Reactive Power Compensation of Transmission Lines. *Power*, pages 1–14, 2005.

[56] Kevin Schönleber, Carlos Collados, Rodrigo Teixeira Pinto, Sergi Ratés-Palau, and Oriol Gomis-Bellmunt. Optimization-based reactive power control in HVDC-connected wind power plants. *Renewable Energy*, 109:500–509, 2017.

[57] G. Daelemans, K. Srivastava, M. Reza, S. Cole, and R. Belmans. Minimization of steady-state losses in meshed networks using VSC HVDC. In *2009 IEEE Power & Energy Society General Meeting*, pages 1–5. IEEE, 7 2009.

[58] Phil S. Jones and Colin C. Davidson. Calculation of power losses for MMC-based VSC HVDC stations. *2013 15th European Conference on Power Electronics and Applications, EPE 2013*, (Mmc):1–10, 2013.

[59] R. Nakagawa, T. Funaki, and K. Matsuura. Installation and control of cycloconverter to low frequency AC power cable transmission. In *Proceedings of the Power Conversion Conference-Osaka 2002 (Cat. No.02TH8579)*, volume 3, pages 1417–1422. IEEE, 2002.

[60] Yongnam Cho, George J. Cokkinides, and A. P. Meliopoulos. LFAC-transmission systems for remote wind farms using a three-phase, six-pulse cycloconverter. In *2012 IEEE Power Electronics and Machines in Wind Applications*, pages 1–7. IEEE, 7 2012.

[61] Jonathan Ruddy, Ronan Meere, and Terence O'Donnell. *A comparison of VSC-HVDC with low frequency AC for offshore wind farm design and interconnection*, volume 80. Elsevier B.V., 2015.

[62] Max Alexander Parker and Olimpo Anaya-Lara. Cost and losses associated with offshore wind farm collection networks which centralise the turbine power electronic converters. *IET Renewable Power Generation*, 7(4):390–400, 7 2013.

[63] Christoph Buchhagen, Christian Rauscher, Andreas Menze, and Jochen Jung. BorWin1 - First Experiences with harmonic interactions in converter dominated grids. *International ETG Congress 2015; Die Energiewende - Blueprints for the new energy age*, pages 27–33, 2015.

[64] L. Harnefors, L. Zhang, and M. Bongiorno. Frequency-domain passivity-based current controller design. *IET Power Electronics*, 1(4):455, 2008.

[65] Jörg Dannehl, Friedrich Wilhelm Fuchs, Steffan Hansen, and Paul Bach Thøgersen. Investigation of Active Damping Approaches for PI-Based Current Control of Grid-Connected Pulse Width Modulation Converters With LCL Filters. *IEEE Transactions on Industry Applications*, 46(4):1509–1517, 7 2010.

[66] Rafael Pena-Alzola, Marco Liserre, Frede Blaabjerg, Martin Ordonez, and Tamas Kerekes. A Self-commissioning Notch Filter for Active Damping in a Three-Phase LCL -Filter-Based Grid-Tie Converter. *IEEE Transactions on Power Electronics*, 29(12):6754–6761, 12 2014.

[67] H. Saad, S. Dennetière, and B. Clerc. Interactions Investigations between Power Electronics Devices Embedded in HVAC Network. In *13th IET International Conference on AC and DC Power Transmission (ACDC 2017)*, pages 55 (7 .)–55 (7 .). Institution of Engineering and Technology, 2017.

[68] IEEE Subsynchronous Resonance Working Group. Reader's guide to subsynchronous resonance. *IEEE Transactions on Power Systems*, 7(1):150–157, 1992.

[69] Khaled Mohammad Alawasa, Yasser Abdel Rady Ibrahim Mohamed, and Wilsun Xu. Active mitigation of subsynchronous interactions be-

tween PWM voltage-source converters and power networks. *IEEE Transactions on Power Electronics*, 29(1):121–134, 2014.

[70] Kala Meah and Sadrul Ula. Comparative evaluation of HVDC and HVAC transmission systems. *2007 IEEE Power Engineering Society General Meeting, PES*, pages 1–5, 2007.

[71] Gregory F. Reed, Hashim A. Al Hassan, Matthew J. Korytowski, Patrick T. Lewis, and Brandon M. Grainger. Comparison of HVAC and HVDC solutions for offshore wind farms with a procedure for system economic evaluation. *2013 IEEE Energytech, Energytech 2013*, 2013.

[72] Hao Chen, Michael H. Johnson, and Dionysios C. Aliprantis. Low-Frequency AC Transmission for Offshore Wind Power. *IEEE Transactions on Power Delivery*, 28(4):2236–2244, 10 2013.

[73] Y. Tang, L. Ran, P.B. Wyllie, O. Alatise, J. Yu, and X.M. Wang. Offshore low frequency AC transmission with back-to-back modular multilevel converter (MMC). In *11th IET International Conference on AC and DC Power Transmission*, pages 046 (8 .)–046 (8 .). Institution of Engineering and Technology, 2015.

[74] Marc Cheah-Mane. Offshore Wind Integration through High Voltage Direct Current Systems. (June), 2017.